Flow in elastic networks subject to pulsatile forcing

Laia González Mena
Facultat de Física, Universitat de Barcelona, Diagonal 645, 08028 Barcelona, Spain.

Advisors: Ignacio Pagonabarraga & Eugenia Corvera Poiré
Facultat de Física, Universitat de Barcelona, Diagonal 645, 08028 Barcelona, Spain; and
Departamento de Física y Química Teórica, Facultad de Química,
Universidad Nacional Autónoma de México, Ciudad de México, 04510 Mexico.

Abstract:
The hemodynamics of a vascular vessel network can be affected by the presence of obstructions. We present a theoretical analysis of the effect that obstructions have on a vessel network under pulsatile inlet pressure, and analyze the importance of the level in which obstructions occur. The elasticity of the vessels is implemented following a recently developed model. Flow and pressure along the network are calculated for a network of equal vessels and for a network that follows Murray's law for radii. The effect of obstructions is evaluated in terms of an effective response, which relates the pressure difference, between the inlet and the outlet of the network, with the blood flow. Our calculations reveal that results obtained for a rigid network and those obtained by taking into account the elasticity of the vessel walls, are qualitatively different. The response of the network when a certain degree of obstruction is present is highly dependent on the level at which the obstructions occur.

I. INTRODUCTION

The vascular system of mammals is of great complexity, therefore sophisticated models are needed to understand the impact of phenomena such as obstructions, stenosis or vessels suppression. The flow at the vicinity of a point where an obstruction occurs as well as the pressure waveforms can be predicted for a concrete morphology[1]-[3].

However, a tree-like network model can be used to study the effect that obstructions have over the whole network, [4],[5]. In several regions, nature provides a wide variety of tree-like structured networks, such as successive bifurcations of large arteries that irrigate the limbs or the microvasculature that irrigates the eyes. At the characteristic frequencies of blood flow, blood exhibits properties of a viscoelastic fluid, with a viscosity and a relaxation time approximately constant, which allows treating it as a Maxwell fluid.

The effect of obstructions on a rigid vessel network under inlet pulsatile pressure can be obtained analytically for rigid vessel networks, [6]. The effective response of the network, which is related with its resistance to flow, is obtained to be a function of the morphology of the network, the fluid properties and frequency.

The presence of obstructions hinders fluid flow, and its impact depends on the position of the obstruction within the network and on the network morphology. For example, for equal vessel networks obstructions have a stronger effect when located at the network entrance. On the other hand, for a network that follow Murray's law, the effect is stronger when they are located at the outlet of the network.

For a rigid network, the effect of obstructions can be quantified in terms of a global relation for the effective response of the network [6], introduced by [4]. The effective response gives a relation between the total pressure drop across the network and the total flow, which can be calculated in terms of the network morphology, and is independent of the pressures imposed at the boundaries. A new model for the flow along a vascular vessel which includes the elasticity of the vessel walls has been developed recently[7]. The model leads to a linear system of equations in frequency domain that predicts the flow and pressure along a vessel network. This new model has been validated with 3D models and uses *in-vivo* measured inflow as a boundary condition.

The aim of this project is to analyse the flow and pressure of a vascular vessel network in the presence of obstructions by taking into account the elasticity of the vessels. We first consider a symmetrically bifurcating elastic vessel network without obstructions and characterize the flow and pressure along the whole network. An oscillatory pressure at the inlet and zero pressure at the outlet is applied. We compare the flow properties in such a network with the ones in a network of equal morphology but composed of rigid vessels. An effective response of the network to the pulsatile forcing, which relates the flow along the network with the pressure gradient, is defined as a generalization of the effective dynamic response of a rigid network[5]. Those responses are used as reference to evaluate the impact that obstructions have. We analyse the effect of obstructions when placed at different levels of the network. Two types of networks are considered: a first case in which all vessels are identical and a second case, in which radii are given by Murray's law.

II. METHODS

A. Network and obstructions models

We use a model which has been recently introduced in order to study viscoelastic flow through a network of tubes [4]. It consists of a tree-like network in which vessels bifurcate always into identical vessels in such a way that, at each bifurcation step, changes of the vessels radii and lengths are allowed. Vessels belonging to the same level are labelled with the same index and have the same radius and length. Counting starts at the outer level, consisting on a main branch and continues to the inner levels, resulting of consecutive bifurcations. The network is characterized, therefore, by the number of levels, N, and the cross-sectional area, A^i, and length, l^i of each level i.

We consider obstructions to occur at half of the vessels at a given level of the network, n. Although this choice is not realistic for blood vessel networks, it provides a systematic way of comparing equivalent obstructions at different levels

In the medical and biological literature, obstructions are characterized by the fraction, f, of cross sectional area which is obstructed. Accordingly to this notation, the obstructed vessels have a cross sectional area $A^n_{obs} = (1-f)A^n$ and an effective radius $r^n_{obs} = \sqrt{(1-f)r^n}$, where A^n and r^n are the area and the radius of the unobstructed vessels of level n respectively. Given the symmetry of the network, flow through the whole network can be characterized by considering two different types of paths. An *unobstructed path*, which goes from the first to the last level without going through the obstruction, and an *obstructed path*, in which an obstructed vessel is crossed at some point. We refer to this two types of paths with subindices *unobs* and *obs* respectively. A scheme of the network can be seen in Fig. 1.

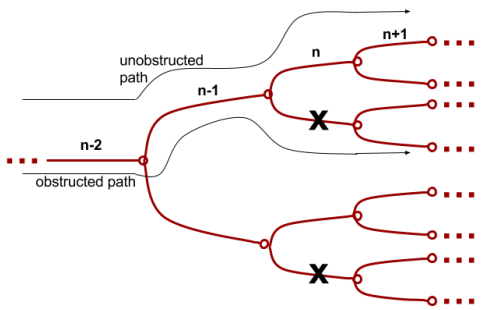

FIG. 1: Scheme of a network with obstructions at level n.

B. Mathematical method: GDEM

The mathematical model used is the GDEM (Generalized Darcy's Elastic Model) [7],[8]. It is based on a generalized Darcy's model for rigid vessels, and it gives equations for the flow and pressure along a vessel network.

Each blood vessel is modelled as a deformable impermeable tube of cylindrical shape. Blood is considered to be a Maxwellian fluid [9] of density ρ, viscosity η and relaxation time t_r. Non-slip boundary conditions are imposed at the average wall position, r. The flow, $\hat{q}$, in frequency domain, is given by a dynamic Darcy's law for a Maxwellian fluid. Such flow is defined as a velocity averaged over the cross sectional area, A, times this cross sectional area, A, and it is given in eq. (1) .

$$\hat{q} = -\frac{AK(\omega)}{\eta}\frac{\partial \hat{p}}{\partial x}. \tag{1}$$

Here, $K(\omega) = -\frac{\eta}{i\omega\rho}\left[1 - \frac{2J_1(\beta r)}{\beta r J_0(\beta r)}\right]$ is the dynamic permeability, a measurement of the resistance to blood flow. J_0 and J_1 are Bessel functions of order 0 and 1 respectively and $\beta^2 = \frac{\rho}{\eta}(t_r\omega^2 + i\omega)$. Hats over hemodynamic quantities denote their Fourier transforms.

The second assumption is that vessel walls are linear elastic tubes which follow Hooke's law. This assumption gives an expression relating changes in pressure with changes in the cross sectional area,which coupled to the axial velocity by conservation of mass leads to eq. (2)

$$-i\omega C\hat{p} + \frac{\partial \hat{q}}{\partial x} = 0. \tag{2}$$

$C = \frac{3\pi r^3}{2Eh}$ is the vessel compliance, where E is the Young modulus and h is the vessel wall thickness. E is calculated using

$$E = 3\rho c^2 r/(2h), \tag{3}$$

being c the pulse wave velocity, given (in m/s) by the empirical relationship $c = 13.3/(2r)^{0.3}$ [10], where r measured in mm. The rigid limit is recovered making $C = 0$.

Eqs. 1 and 2 yield an harmonic oscillator equation for pressure in frequency domain,

$$\frac{\partial^2 \hat{p}}{\partial x^2} = -k_c^2 \hat{p}, \tag{4}$$

with $k_c^2 = \frac{i\omega C\eta}{AK(\omega)}$. Solving eq.4 with boundary conditions p_{in} and p_o for inlet and outlet pressure respectively yields the following analytical expression for the pressure:

$$\hat{p}(x) = \hat{p}_{in}cos(k_c x) + \frac{\hat{p}_o - \hat{p}_{in}cos(k_c l)}{sin(k_c l)}sin(k_c x), \tag{5}$$

which substituted in eq. (1) leads to an analytical expression for the flow:

$$\hat{q}(x) = M\left(\hat{p}_{in}sin(k_c x) - \frac{\hat{p}_o - \hat{p}_{in}cos(k_c l)}{sin(k_c l)}cos(k_c x)\right), \tag{6}$$

where $M^2 = i\omega CAK(\omega)/\eta$.

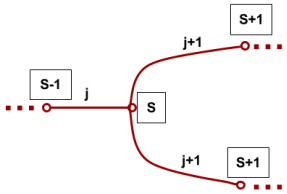

FIG. 2: Nodes connection.

Now we consider a network composed by different vessels connected, each of them fulfilling eqs. (1)-(7). A system of equations can be constructed using eq. (6) for the flow at each level and imposing flow conservation at the nodes. We define a node S as the mathematical point where bifurcation from level j to level $j+1$ happens as shown in Fig. 2. Flow conservation is expressed as $\hat{q}_o^j = 2\hat{q}_{in}^{j+1}$. Making use of eq. (6):

$$M^j\left(\frac{\hat{p}^{[S-1]} - \hat{p}^{[S]}cos(k_c^j l^l)}{sin(k_c^j l^l)}\right) = -2M^{j+1}\left(\frac{\hat{p}^{[S+1]} - \hat{p}^{[S]}cos(k_c^{j+1} l^{j+1})}{sin(k_c^{j+1} l^{j+1})}\right), \tag{7}$$

where $p^j(x)$ and $q^j(x)$ denote pressure and flow of a vessel of level j, sub indices in and o indicate the inlet and the outlet of the vessel respectively and $p^{[S]}$ indicates pressure at node S. Eq. (7) must be fulfilled in all the nodes of both the obstructed and the unobstructed path. At $j = n-1$, vessels after the bifurcation have different effective cross sectional area due to the obstruction in one of them. Therefore, we must consider that the flow is different between them: $\hat{q}_o^j = (\hat{q}_{in}^{j+1})_{unobs} + (\hat{q}_{in}^{j+1})_{obs}$, which gives:

$$M^{n-1}\left(\frac{\hat{p}^{[S-1]} - \hat{p}^{[S]}cos(k_c^{n-1} l)}{sin(k_c^{n-1} l^{n-1})}\right) = -\left[M^n\left(\frac{\hat{p}^{[S+1]} - \hat{p}^{[S]}cos(k_c^n l^n)}{sin(k_c^n l^n)}\right)\right]_{unobs} - \left[M^n\left(\frac{\hat{p}^{[S+1]} - \hat{p}^{[S]}cos(k_c^n l^n)}{sin(k_c^n l^n)}\right)\right]_{obs}, \tag{8}$$

where M^n and k_c^n of the obstructed path are computed using the effective radius r_{obs}^n. Application of eqs. 7 and 8 to the 2N-n-1 different nodes of the system (n-1 before the obstruction and twice N-n-1 from the obstruction to the outlet, both for the obstructed and unobstructed bath) and taking into account that $p^{[S-1]} = p_{in}$ for at first node and that $p^{[S+1]} = p_o$ at the last, leads to a linear system of equations for pressure at the nodes in the Fourier domain. $p_{in} and p_o$ are known. We solve the system numerically for different frequencies ω. Once the pressure at the nodes is known, pressure and flow as a function of the position, x, for each vessel can be obtained by making use of eqs. 5 and 6.

The boundary conditions are: pulsatile forcing at the inlet and zero pressure at the outlet:

$$p_{in}(t) = \Delta p^0 cos(\omega_0 t) \tag{9}$$

$$p_o(t) = 0, \tag{10}$$

where Δp^0 is the magnitude of the oscillations at the inlet and ω_0 is its angular frequency of oscillation.

C. Parameters of the networks

Hemodynamics through a vessel network is highly affected by its morphology. We consider two models for the networks.

The first model that we consider has all the same length and cross-sectional area in all the vessel, independently of the level at which they are located. We refer to this network as the *equal vessel network*. It could be of interest for microfluidic elastic tubes studies. Furthermore, it can be found in the vascular system of mammal, at the arteriole level. We take a network of 11 levels with vessels of the size of the typical arterioles of a dog, of radius $r = 10^{-5}m$ and length $l = 2\cdot 10^{-3}m$ [16]. In order to appreciate the effect of the elasticity of the vessel walls, we take a high enough elasticity and refer to it as the *elastic case*, with a Young modulus $E = 10^5 Pa$. We also consider the elasticity that such network would have in a biological system, according to eq. (3). Young modulus, E, of the vessel walls in biological conditions decreases with r, according to eq. (3) and refer to it as the *real case*. However, E is obtained to be of the order 10^7 Pa, and at such low elasticity the hemodynamics are basically those of a rigid network. We also compute the *rigid case* as a reference. We show graphics for both the rigid and the elastic cases, the real case is omitted, although the differences with the rigid case are commented.

The second model is a network which follows Murray's law. It considers that, at each node, when a vessel (which is called the *parent* vessel and have radius r_p) bifurcates in two vessels (called the *daughter* vessels of radii r_{d1} and r_{d2}), r_p, r_{d1} and r_{d2} fulfil the relation $r_p^2 = r_{d1}^2 + r_{d2}^2$. In our case, in which the daughter vessels are equal, making $r_{d1} = r_{d2}$ leads for the following relation

$$r_i = \left(\frac{1}{2}\right)^{(i-1)/3} r_1. \tag{11}$$

Murray's law was first derived from minimization of the energy needed in order to keep circulating in a vascular

system [11]. Later physiological studies have validated the agreement of Murray's in vascular systems of mammals and even for water transport in plants [12]-[14]. We study a network that goes from the aorta to the capillaries taking the radii and length of a typical dog, which needs of N =29 levels: $r_1 = 5 \cdot 10^{-3}$m, $r_N = 8 \cdot 10^{-6}$, $l_1 = 0.4$ m, $l_{29} = 10^{-3}$ m. For the lengths of the vessels, we adjust a power law that goes from l_1 to l_{29}.

We use parameters of normal dog blood [16]: $\rho = 1050kg/m^3, \eta = 1.5 \cdot 10^{-2}kg/(m \cdot s), t_r = 10^{-3}s$. We work at the frequency of the resting heart rate of a dog, $\omega_0 = 2\pi 1.5Hz$.

D. Total flow

We define the total flow at a given position as the sum of the flows that go through all the vessels at that position. For example, at level 3 in the network, we have 4 vessels. Accordingly, the total flow at the inlet of the third level, is four times the flow at the inlet of a vessel of the third level. In general, for level j, the total flow at position x is

$$Q_j(x) = 2^{j-1} q^j(x), \tag{12}$$

where $q^j(x)$ is the flow that goes through a single vessel of level j. The total flow is a quantity that must be continuous in order to fulfill mass conservation. In the rigid case, it must be, in addition, constant along the whole network, given that it is constant along every vessel.

E. Effective response function

In rigid networks, flow along the whole network is commonly described by means of the effective dynamic response function, $\chi(\omega)$, which is a measure of the flow that goes through the network in relation with the pressure difference between the inlet and the outlet. It is introduced by integration of the Darcy's law, as we explain next.

Integration of eq. (1) along a vessel leads to $\hat{q}_i = -\frac{K_i A_i \Delta \hat{p}_i}{\eta l_i}$ (for a rigid network, eq. (2) becomes $\nabla \hat{q}_i = 0$, so q_i is constant along x) . Taking into account that the total pressure drop of the whole network is given by the sum of partial pressure drops at each level and that flow is conserved ($q_i = 2q_{i+1}$), the following relation is obtained:

$$\hat{q}_1 = -\frac{\chi(\omega)\Delta\hat{p}(\omega)}{\eta L}, \tag{13}$$

where χ is defined as

$$\frac{1}{\chi} = \frac{1}{L}\sum_{i=1}^{N} \frac{l_i}{2^{i-1} A_i K_i}. \tag{14}$$

q_1 of eq. (13) is the flow at the inlet, but given flow conservation and that flow is constant along each vessel it is the total flow at any of the network, $q_1 = Q_i \equiv 2^{i-1} q_i$.

For a general elastic network, we can still use a global response function relating flow and pressure difference by making a remark on the flow. However, eq. 14 does not hold anymore. In eq. (13), q_1 is a good global measure, since the total flow, Q_i is constant through the whole network. On an elastic network, however, Q is not constant anymore. We use instead of q_1, the average flow along the network:

$$< \hat{Q} > = \frac{1}{L}\int_0^L \hat{Q}(x)dx = \frac{1}{L}\sum_{i=1}^{N}\int_0^{l_i} 2^{i-1}\hat{q}_i(x)dx =$$

$$= \frac{1}{L}\sum_{i=1}^{N} 2^{i-1} l_i < \hat{q}_i >,$$

where $< \hat{q}_i >= -\frac{A_i K_i}{\eta l_i}\Delta\hat{p}_i$, using eq. (7).

We define the global response function for an elastic network as:

$$\chi = -\frac{\eta L < \hat{Q} >}{\Delta\hat{p}}. \tag{15}$$

In the limit of a rigid network, eq. (16) coincides with the deffinition for a rigid network in eq. (13).

We also introduce a measure of the heterogeneity of the flow along the network, $\sigma(\chi)$.

$$\sigma(\chi) = -\frac{\eta L}{\Delta\hat{p}}\sqrt{\sum_{i=1}^{N}(< \hat{Q}_i > - < \hat{Q} >)^2}, \tag{16}$$

which is a measure of how far is a network from its rigid equivalent. For a rigid network, $\sigma(\chi) = 0$. The heterogeneity is measured in the same units as χ, so the ratio $\sigma(\chi)/\chi$ is the relative uncertainty in the measure of χ.

III. EFFECT OF ELASTICITY ON AN UNOBSTRUCTED NETWORK

In Figs. 3a, 3c we plot, for an equal vessel network, the pressure profiles for the rigid and the elastic cases, respectively. Each line corresponds to a different time, which is measured as function of the period of oscillation of the inlet pressure, $T = 2\pi/\omega_0$, and each color to a different level in the network. In both cases, the pressure profile goes to zero when approaching the outlet, decaying faster near the inlet. At $t = 0$, in 3c, a little bump is observed near the inlet and the lines at each level are not strictly straight. In Fig. 3a, however, pressure is always either monotonically increasing or decreasing from the inlet to the outlet, depending on the time, and the pressure gradient along each level is constant. Figs. 3b, 3d show the time evolution of the pressure. Each color corresponds to a different node, located at the corresponding color

. **Equal vessel network**

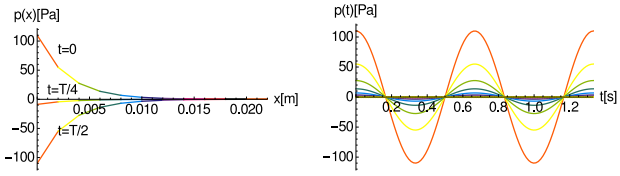

(a) Rigid. p(x) (b) Rigid. p(t)

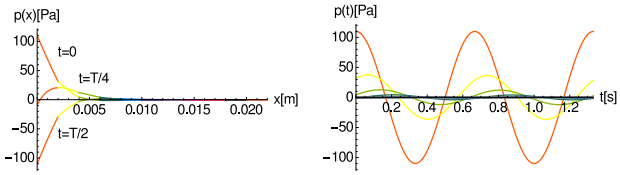

(c) Elastic. p(x) (d) Elastic. p(t)

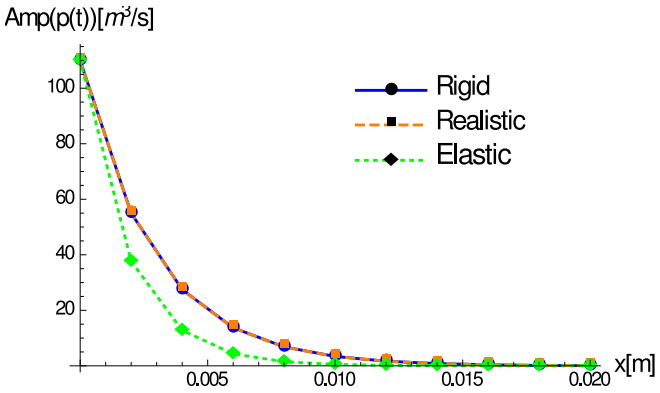

(e) Amplitude of p(t)

FIG. 3: Pressure for an equal vessel network. At the top, (a-b), for a rigid network (and the realistic case, as it is deffined in section II.C). Below, (c-d), for an elastic network. (a), (c): pressure profile along the network at three different times. (b), (d): time evolution of the pressure at the inlet and each node. Each color corresponds to the node located at the corresponding position in (a) and (c). (e): Amplitude of the oscillations of the pressure as a function of the position for the rigid, real and elastic cases in a blue solid, orange dashed and green dotted lines, respectively.

Network that follows Murray's law

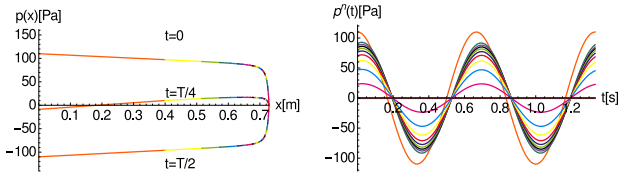

(a) Rigid. p(x) (b) Rigid. p(t)

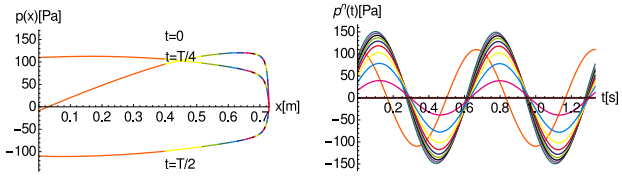

(c) Elastic. p(x) (d) Elastic. p(t)

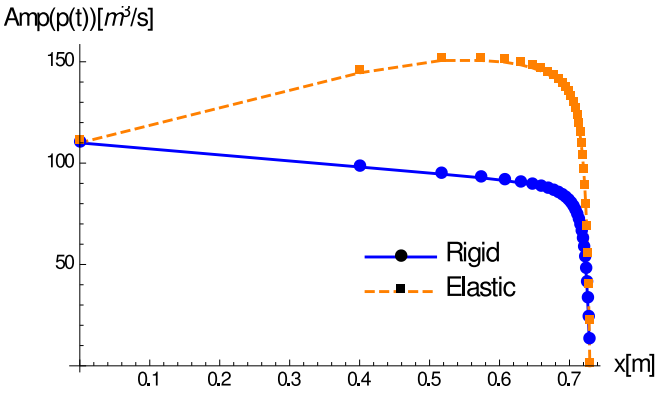

(e) Amplitude of p(t)

FIG. 4: Same graphics for pressure as in Fig.3 for a Murray's network.

in the pressure profiles. Fig 3d shows a phase difference between the oscillations of the pressure, whereas in Fig 3b all nodes oscillate in phase. In Fig.3e, we compare the amplitude pressure oscillations along the network for the three different cases of elasticity. They all start at 110Pa, in accordance with the inlet boundary condition and rapidly decay to zero. The elastic case decays faster than the elastic and the real cases, which are coincident. The real case has not been represented in Figs. 3a-d, since the effect the elasticity has such a low impact that no difference can be appreciated from the rigid case. We conclude, that the effect of the elasticity on the pressure is a faster decay along the network and a difference of phase between its oscillations at different points of the network.

In Fig. 4, we make the same analysis as in Fig. 3 for a Murray's network. Some of the effects of the elasticity on a Murray's network are the same as those observed for the equal vessel one. A curvature of the lines along a vessel in Fig. 4c instead of straight lines for the rigid case in Fig. 4a and a phase difference of the oscillations at the different nodes in 4d instead of the oscillations in phase of the rigid case in 4b. Some other features of the pressure along a Murray's network differ from those of the equal vessel one. Fig. 4e shows that the amplitude of the pressure along a rigid network decays very slowly with a constant slope with x along the first levels of the network, which is about the 90% of the total length of the network, and that it drops fast to zero at the other levels. The curve for the elastic case of the pressure oscillation amplitude, however, is is increasing for the two first levels and then slowly decreasing, showing a maximum of the pressure amplitude between the second and the third levels. At the very end of the network, pressure amplitude sharply goes to zero, in the same way as for

the rigid case.

Equal vessel network

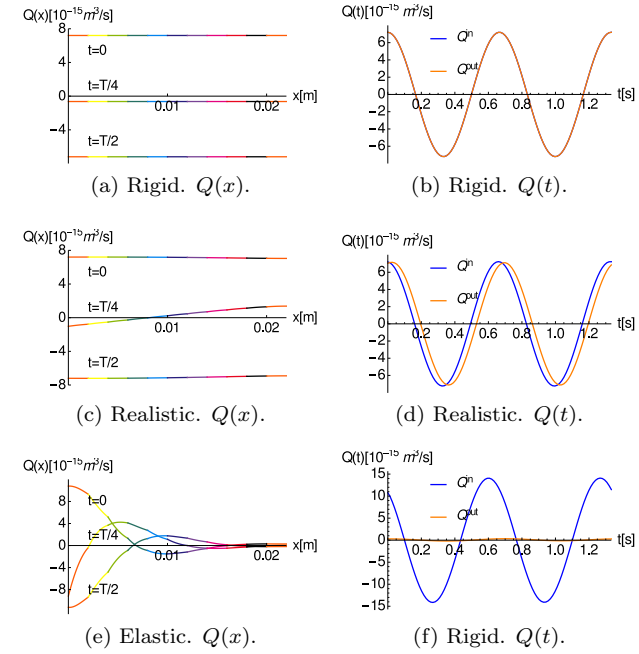

(a) Rigid. $Q(x)$. (b) Rigid. $Q(t)$.

(c) Realistic. $Q(x)$. (d) Realistic. $Q(t)$.

(e) Elastic. $Q(x)$. (f) Rigid. $Q(t)$.

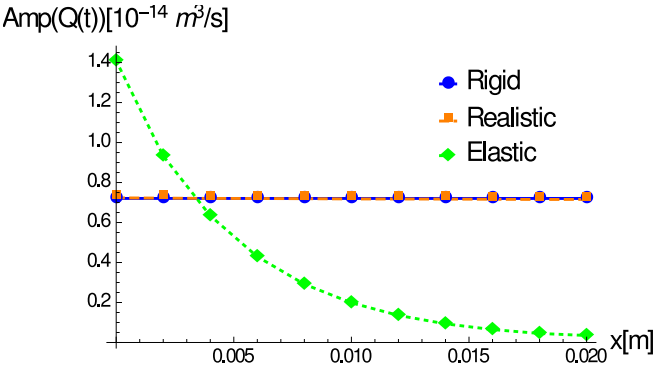

(g) Amplitude of $Q(t)$.

FIG. 5: Total flow, Q, of an equal vessel network (eq. (12)). (a-b), for a rigid network,, (c-d), for a realistic network, (e-f) for an elastic network. (a,c,e): Q profile along the network at three different times. (b,d,f): time evolution of the total flow at the inlet (blue) and at the outlet (orange) of the network. (g): Amplitude of the oscillations of Q as a function of the position for the rigid, real and elastic cases in a blue solid, orange dashed and green dotted lines, respectively.

In Fig. 5, we present graphics for the total flow, Q, for the equal vessel network. In Figs. 5a, 5c, 5e we plot the profile of Q for the rigid, the realistic and the elastic cases, respectively. Each line corresponds to a different time and each color to a different level in the network. For the rigid case in Fig. 5a, Q is constant along the network at any time, consistently with theory. For the elastic case in 5e, conversely, Q decays to nearly zero after some oscillations. The realistic case differs slightly from the rigid case, showing a slope for $t = 0$. Figs. 5b, 5d, 5f show the time evolution of Q at the inlet, in blue, and the outlet in orange. In Fig. 5b, for the rigid case, Q at the inlet and the outlet coincide exactly. In Fig. 5f, however, Q at the inlet is larger than in the rigid case and at the outlet oscillates very close to zero (notice the orange line almost overlapping the x axis). In fig. 5f a little difference of phase between the inlet and the outle total flow can be appreciated. In Fig. 5g, the amplitude of the oscillations of Q along the network are compared, for the rigid and the elastic cases. Total flow amplitude at the inlet of the elastic network is about the double than in the rigid one and it decays monotonically, more rapidly near the inlet and softly when approaching the outlet. For the rigid and the real cases, however, total flow amplitude is kept constant along the whole network. Elasticity in equal vessel networks leads to absorption of the incoming pressure wave rather than transmitting it.

Network that follows Murray's law

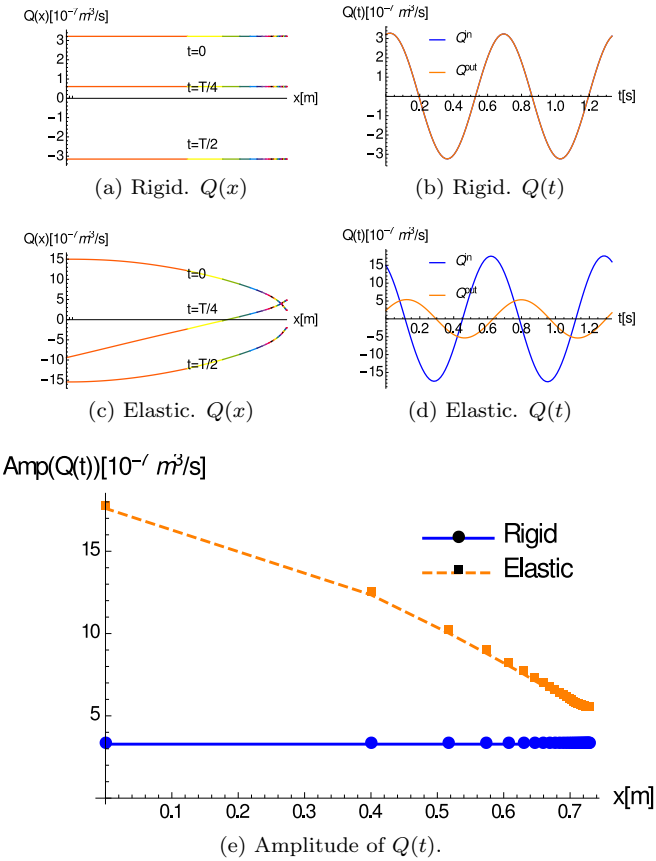

(a) Rigid. $Q(x)$ (b) Rigid. $Q(t)$

(c) Elastic. $Q(x)$ (d) Elastic. $Q(t)$

(e) Amplitude of $Q(t)$.

FIG. 6: Same graphics for the total flow, Q, as in Fig. 5 for a Murray's network.

In Fig. 6, we make the same analysis as in Fig. 5 for a Murray's network. As well as for the pressure, some of the effects of the elasticity on the total flow of a Murray's network are the same as those observed on the equal

vessel one and some are different. For the rigid case, Q profile is constant along the network in Fig. 6a, whereas for the elastic case, in Fig. 6c, the lines curve towards the x axis when approaching the outlet. The time evolution of Q of the rigid network (Fig. 6b) at the inlet and the outlet of the network coincide. For the elastic network, however, Fig. 6d, the amplitude of oscillation and the inlet is larger than at the outlet and there is a phase difference between them. The main difference with respect to the equal vessel network can be seen in Fig. 6 (e). There, the amplitude of the oscillations of the total flow decays approximately linearly with x and remains always larger than in the rigid case.

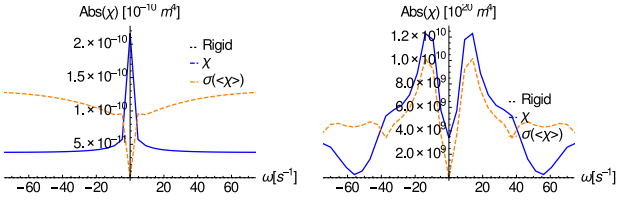

(a) Equal vessel (b) Murray

FIG. 7: Absolute value of $\chi(\omega)$ for the equal vessel network, (a), and the unobstructed network, (b). χ is presented in solid blue lines and $\sigma(\chi)$ is dashed orange lines. χ for a rigid network is also included in dotted black lines as a reference.

In Fig.7, the absolute value of the effective response function is presented for the equal vessel network, (a), and for Murray's, (b). For both networks, the curve for the elastic network coincides with the rigid case at $\omega = 0$, where $\sigma(\chi) = 0$, which is consistent with the equations. In Fig.7a, $\sigma(\chi)$ is larger than χ except for low frequencies (below $5s^{-1}$), and in Fig.7b, for the Murray's network is of the order of χ. In both cases such a large σ reveals a high heterogeneity of the flow along the network. For the equal vessel network, Fig.7a, except for those low frequencies at which the network behave similarly to its corresponding rigid network, the χ becomes nearly constant with ω and remains lower than that of a rigid network. σ grows smoothly, being several times larger than χ.

For a Murray's network, Fig.7b, the behaviour of both χ and $\sigma(\chi)$ rapidly differs from the rigid case with ω. Both χ and $\omega(\chi)$ are higher than χ of the rigid network and oscillate with omega. Their highest value is found between $\omega = 10s^{-1}$ and $\omega = 20s^{-1}$.

IV. EFFECT OF OBSTRUCTIONS

We evaluate the response function of the network,χ and its root mean square deviation (RMSD), $\sigma(\chi)$. χ is given in terms of the response of the same unobstructed network, χ_{un} and $\sigma(\chi)$ in terms of χ, so that it can be interpreted as a relative error. Both quantities are evaluated at frequency ω_0.

In Fig. 8, we present the results for the equal vessel network. Since the imaginary part of the response function is one order of magnitude lower than the real part, we focus on the real part of χ and σ. The points, joined by solid lines, belong to the elastic network and the dashed lines to the rigid one. Colours blue, orange and green correspond to a level of obstruction, f, of the $30\%, 60\%$ and 90%, respectively.

Equal vessel network with obstructions

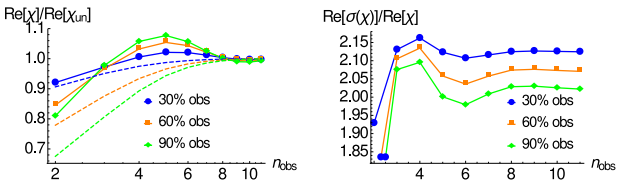

(a) (b)

FIG. 8: Real part of the response function, χ, in (a); and its relative error, σ/χ, in (b), for an obstructed elastic network of equal vessels as function of the level at which obstructions occur. Colours blue, orange and green correspond to $30\%, 60\%$ and 90% of obstructed cross section, respectively. Dashed lines in (a) correspond to the rigid case. $\sigma(\chi)/\chi$ of the elastic network. For a rigid network, $\sigma(\chi)/\chi = 0$, so the rigid case is not represented in (b).

In Fig. 8 (a), we see that when obstructions are placed before the fifth level, χ increases with n_{obs}. It is remarkable that when obstructions are placed in the middle levels,5th and 6th, the response function is larger than that of an unobstructed network. Conversely, when obstructions are placed at the inner levels, above 5, $Re[\chi]/Re[\chi_{un}]$ decays with n_{obs} to a value near 1. The effect of obstructions is higher the higher the percentage of obstruction is and therefore the curve for $f = 90\%$ is always the furthest from 1, i.e. it is the highest when $Re[\chi]/Re[\chi_{un}] > 1$ and the lowest when $Re[\chi]/Re[\chi_{un}] < 1$. Lines for different f cross at some points, near $n_{obs} = 3$ and $n_{obs} = 8$. When obstructions are located between the 4th and the 8th levels, χ of an elastic network is larger than without, in opposition to the rigid network, in which χ/χ^{un} is always less than 1. In Fig. 8 (b), we see that $\sigma(\chi)/\chi$ is about twice the value of χ. Given this high heterogeneity of the response along the network, the average response of the network could not be representative of what happens at each level and further study focussing on local response may be of importance to understand the physical origin of the maximum.

In Fig. 9, the same analysis is done for the Murray's network. In this case, the real and the imaginary part of the response function happen to be of the same order of magnitude and to have a similar dependence on n_{obs}. We present therefore the absolute value of χ and σ, being representative of both their real and imaginary parts.

Results for the 10% of obstructions and for the 60% of obstructions are plotted in Figs. 9 (a-b) and (c-d) respectively. The shape of the curves in (a) and (c) are similar, but in (c) the effect of the obstructions is stronger than in (a) by a factor 10. χ is, in general, lower than χ_{un}. χ/χ_{ub} exhibits a peak at level 20 and stays close to 1 until the deepest levels, where obstructions have their least impact. Therefore, the effect of the obstructions is highest when they are placed at the outer levels. When they are close to level 20, the average response is mainly the same as when there are no obstructions. It also coincides with a peak of $\sigma(\chi)$, Fig. 9 (b) and (d). Therefore, at level 20 is where χ is closest to χ_{un} and also where the response of the network is more heterogeneous. The effect of a rigid network is opposite: obstructions have their greatest effect when increasing n_{obs}, being maximum at the deepest level for $f = 10\%$ and near level 23 for $f = 60\%$. . In Fig. 9 (b) and (d) we see that the value of σ/χ is between 3.60 and 3.65 for $f = 10\%$ and between 3.5 and 4 for $f = 60\%$.

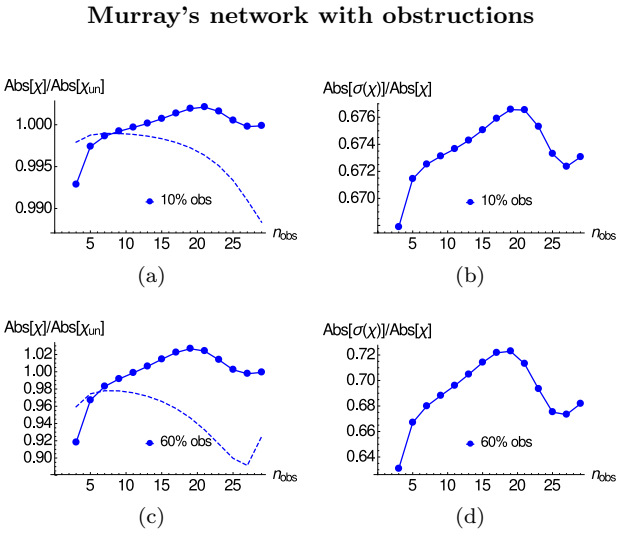

FIG. 9: Absolute value of the response function for an obstructed network that follows Murray's law. (a) and (b): 10% of obstructed cross section, (c) and (d): 60% of obstructed cross section. (a) and (c): $Re[\chi]/Re[\chi_{un}]$. In solid lines with dots the response of an elastic network and in dashed lines the rigid case. (b) and (d): $\sigma(\chi)/\chi$ of the elastic network. For a rigid network, $\sigma(\chi)/\chi = 0$.

In Figs. 10 and 11, we analyse in more detail the impact that the position of the obstruction in the network on the hemodynamics of the network. We take the particular case of n_{obs} at a level near the inlet (at levels 2 and 3 for equal vessels and Murray, respectively) and near the outlet (at levels 10 and 20 for equal vessels and Murray, respectively). We plot the amplitude of oscillation of the pressure of each node and the average flow amplitude of oscillation at each level. Since the flow is reduced at each level due to flow conservation at the bifurcations, we multiply, at each level i, the flow amplitude by a factor 2^{i-1} in order to compare the flow between different levels. Results are presented both along the obstructed and the unobstructed path and they are compared with the corresponding unobstructed network.

From Fig. 8, we know that the equal vessel network has a minimum response for $n_{obs} = 2$. In Fig. 10, the amplitude of oscillation of the pressure at each node, (a), and the average flow amplitude at each level, (b) are presented in logarithmic scale. It is clear that the effect of obstructions on the obstructed path is larger than on the unobstructed path for both pressure, (a), and flow, (b). The effect of the obstruction along the obstructed path is clear in both Fig. 10a and 10b. Pressure and flow along the obstructed path are about one order of magnitude below their values for an unobstructed network. Conversely, the value of those magnitudes along the unobstructed path are over the values of the unobstructed network by less than a factor two. The ratio between the obstructed and the unobstructed path is kept along the levels. In (b), we see that, even though the average total flow does not differ much from the average flow of an unobstructed network, the obstruction has severely hindered flow along the obstructed path.

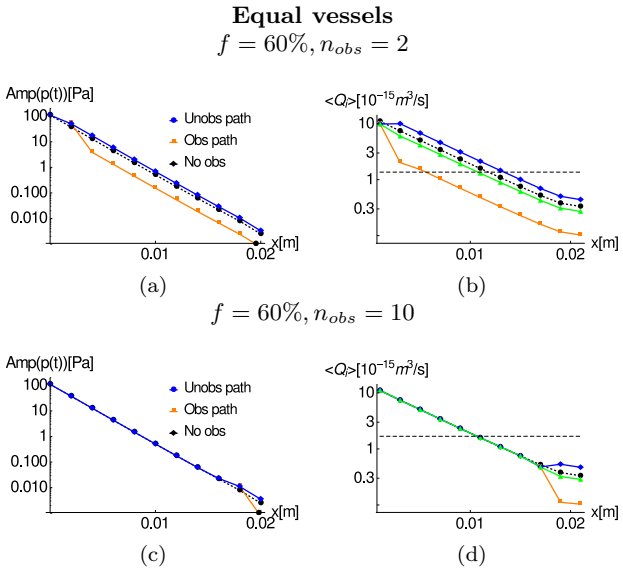

FIG. 10: Pressure and flow profiles of a network of equal vessels for 60% os obstructions at level 2 and level 10, in (a-b) and (c-d) respectively. (a,c): Amplitude of oscillation at each bifurcation. (b,d): amplitude of oscillation of the flow averaged along a vessel of level i multiplied by 2^{i-1}. In blue, the unobstructed path, in orange, the obstructed path and in dotted black lines de case for the same unobstructed network. In (b), the green line corresponds to the average total flow (between the obstructed and the unobstructed paths) and the horizontal dashed black line is the average flow amplitude along the whole network.

For a network that follows Murray's law, we analyse networks with obstructions at two different levels for

$f = 60\%$. At level 3, in Fig. 11, which we know to have the lowest response from Fig. 9, and at level 20, which is the less affected by the obstructions on the average response function. Results are presented in linear scale. Flow and pressure on a network that follows Murray's law is affected by obstructions in a similar way as the equal vessel network is: both the pressure amplitude and the average amplitude flow at each level along the obstructed path differ more from the unobstructed network quantities than the unobstructed network than those quantities along the unobstructed path. Flow and pressure at the obstructed path are diminished and at the unobstructed path are enlarged by the obstructions. The magnitude of the variations, however, is much lower in the Murray's network, i.e for $n_{obs} = 3$ (Fig. 11), pressure is diminished by a factor 0.7 at the obstructed path and enlarged by a factor 1.1 at the unobstructed path with respect to the unobstructed network and similar values are found for the average flow amplitude. It is also noticeable a decrease of the flow amplitude at the outer levels of the network, before the obstruction. Therefore, the effect of the obstructions is not local, but affects the whole network. Notice that the average total flow (Fig. 11 (b), in green) is always below the flow of the unobstructed network.

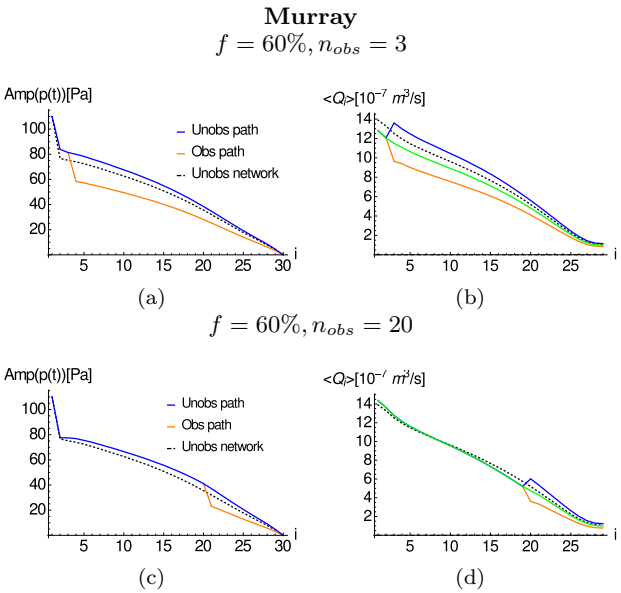

FIG. 11: Same graphics for pressure and flow profiles of a network that follows Murray's law for 60% of obstructions at level 3 and level 20, (a-b) and (c-d) respectively.

V. CONCLUSIONS

Vessel wall elasticity has a profound impact in the pressure and flow distribution along a tree-like network with respect to the rigid case. When an oscillatory pressure is applied at the inlet, the effect of the elasticity on the transmission of the perturbation to the outlet highly depends on the geometry of the network.

If we consider a network of equal vessels, the amplitude of the pressure oscillations along the network drops faster when going to the inner levels than in a rigid network. In the rigid case, the oscillatory flow at the inlet, consequence the inlet pulsatile forcing, is fully transmitted to the outlet, where there is no pressure. On an elastic network, however, flow at the outlet is diminished with elasticity and, for elastic enough networks, no flow oscillations are measured at the outlet, the perturbation has not been transmitted to the outlet. It can be understood as the elasticity of the vessel walls absorbing the energy of the inlet perturbation. Since the pressure has rapidly gone to zero when going deeper in the network, there is no pressure gradient to originate the flow. Elasticity has a strong effect at ranges of elasticity higher than the typical elasticity of the dog arterioles, for example for elastic microfuidic experiments.

For a network that follows Murray's law, in which the outer vessels are wider and longer and their size is reduced when going to the inner levels, the perturbation at the origin is enlarged along the network by elasticity. Pressure oscillations grow when going deeper and they produce an oscillatory flow which is larger along the whole network than if the vessel walls were rigid. Just at the very end of the network, pressure oscillations drop to zero. Flow oscillations of an elastic network of these characteristics are larger at the inlet than at the outlet of the network, they monotonically decrease when going deep across the levels. Therefore, part of the energy of the oscillations at the inlet is absorbed by the elasticity of the vessel walls.

A global response function of an elastic network can be introduced as a generalization of the response function of a rigid network, relating the average flow along the network with the pressure difference at its extremes. Additionally, a measure of the response function heterogeneity along the network, which can be several times larger than the response function itself, complements the information given by the response function.

On a network of equal vessels, the impact of obstructing part of the vessels at a given level is to decrease the response of the network. That effect, is larger the outer the obstruction are and have their lowest effect when they are placed at the innermost level. An elastic network of the same characteristic becomes more affected by the obstructions at the outer level and not as much at the middle and inner ones. It must be taken on account, however, the heterogeneity of the response function along the network.

On a network that follows Murray's law, the behaviour of the response function with the place at which obstructions occur is basically inverted with respect to the same rigid network. Instead of having the largest effect of reducing the response of the network at the inner levels and weakly depending on the place at which they occur at the

outer and middle levels, the response function is monotonically increased with the level at which obstructions are. Therefore, the greatest effect of the obstructions is at the outer levels, in a similar way to the equal vessel network.

Local flow study of the flow along a network with obstructions show that the effect of the obstruction is not local but affect the flow of the whole network. The most affected part is the path after the obstruction, where flow is diminished. Flow along the unobstructed path from the level of the obstruction until the outlet, however becomes enlarged. Finally, flow before the obstruction is also modified, being diminished near the obstruction and enlarged close to the inlet. The equal vessel network has been shown to be more sensible than the Murray's network to the same level of obstruction.

Further study of the impact of obstructions on the network response to a pressure gradient needs to take into account the heterogeneity of the flow along the network. The ratio between flow along the obstructed path and at its corresponding unobstructed network has been found to be constant along the network and could be a starting point for later studies.

Acknowledgments

I thank my advisors Eugenia Corvera Poiré and Ignasi Pagonabarraga for their guidance through the project. I also thank Joaquín Flores Gerónimo and Aimee Torres Rojas for sharing their expertise and for useful discussions, and I thank Carlos and my family for their moral support.

IP and ECP declare that the research leading to these results has received funding from the European Union Seventh Framework Programme (FP7-PEOPLE-2011-IIF) under grant agreement No 301214. ECP acknowledges financial support from CONACyT (Mexico) through project 219584.

[1] N. Stergiopulos, D.F. Young, T.R. Rogge (1992) *Computer simulation of arterial flow with applications to arterial and aortic stenoses.* Journal of Biomechanics, Volume 25, Issue 12, Pages 1477-1488

[2] L. Formaggia, D. Lamponi, M. Tuveri & A. Veneziania *Numerical modeling of 1D arterial networks coupled with a lumped parameters description of the heart.* Computer Methods in Biomechanics and Biomedical Engineering, Volume 9, Issue 5, 2006 .

[3] Alastruey J., Parker K.H., Peiró J., Byrd S.M., Sherwin S.J. (2007) *Modelling the circle of Willis to assess the effects of anatomical variations and occlusions on cerebral flows.* J. Biomech, 40 1794-1805.

[4] Flores J., Corvera Poiré, E.,del Río J.A. $ López de Haro M.*A plausible explanation for heart rates in mammals.* J. Theoretical Biology, 317 (2013) 257-270.

[5] Flores J.,Romero A.M.,Travasso R.D.M. & Corvera Poiré, E. *Flow and anastomosis in vascular netwroks.* J. Theoretical Biology, 317 (2013) 257-270.

[6] Torres Rojas AM, Romero A.M., Pagonabarraga I, Travasso RDM, Corvera Poiré E (2015)*Obstructions in Vascular Networks: Relation Between Network Morphology and Blood Supply.* PLoS ONE 10(6): e0128111. doi:10.1371/journal.pone.0128111

[7] Flores, J., Alastruey, J., & Corvera Poiré, E. (2016). *A novel analytical approach to pulsatile blood flow in the arterial network.* Annals of Biomedical Engineering. 10.1007/s10439-016-1625-3

[8] del Río, J. A., M. López de Haro, and S. Whitaker. Enhancement in the dynamic response of a viscoelastic fluid flowing in a tube. Phys. Rev. E 58, 6323?6327, 1998.

[9] Thurston GB, Henderson NM. *Effects of flow geometry on blood viscoelasticity.* Biorheology, 2006;43(6):729-46.

[10] Reymond P, Merenda F, Perren F, Rfenacht D & Stergiopulos N. *Validation of a one-dimensional model of the systemic arterial tree.* American Journal of Physiology - Heart and Circulatory Physiology (2009) 297; 1. DOI: 10.1152/ajpheart.00037.2009

[11] Murray CD. *The Physiological Principle of Minimum Work: I. The Vascular System and the Cost of Blood Volume.* Proc Natl Acad Sci USA (1926) 12(3):207-14.

[12] Sherman TF. *On connecting large vessels to small. The meaning of Murray's law.*J Gen Physiol. (1981) 78(4):431-53.

[13] Taber LA, Ng S, Quesnel AM, Whatman J, Carmen CJ.*Investigating Murray's law in the chick embryo.* J Biomech. 2001 Jan;34(1):121-4.

[14] KA McCulloh, JS Sperry & FR Adler. *Water transport in plants obeys Murray's law.* Nature 421, 939-942. doi:10.1038/nature01444

[15] Epstein S., Willemet M., Chowienczyk P.J., Alastruey J. *Reducing the number of parameters in 1D arterial blood flow modeling: less is more for patient-specific simulations.* American Journal of Physiology - Heart and Circulatory Physiology Jul 2015, 309 (1) H222-H234; DOI: 10.1152/ajpheart.00857.2014

[16] Nichols WW, O'Rourke MF& Vlachopoulos C. *Theoretical, Experimental and Clinical Principles.* New York: Arnold/Oxford University Press; 1998.

VI. APPENDIX

For an unobstructed network of equal vessels, we find a couple of relations which must be identically fulfilled. The first relation can be obtained by integrating eq. (1) along a trajectory, i.e. integrating over positions along a vessel from the first to the last levels. Continuity of the

pressure at the bifurcations is imposed.

$$< \hat{q} >_{traj} = \frac{1}{L}\sum_{i=1}^{N}\int_0^{l_i} \hat{q}_i(x)dx = \tag{17}$$
$$= -\sum_{i=1}^{N}\int_0^{l_i} \frac{AK(\omega)}{\eta L}\frac{\partial \hat{p}_i(x)}{\partial x}dx = -\frac{KA}{\eta}\frac{\Delta\hat{p}_{TOT}}{L},$$

where $\Delta\hat{p}_{TOT}$ is the pressure difference between the inlet and the outlet of the network, in Fourier domain. Eq. (17) permits to define a quantity: $\chi_1(\omega) = \frac{<\hat{q}>_{traj}/\Delta\hat{p}_{TOT}}{KA/(\eta L)}$ For an unobstructed network, $\chi_1(\omega) = 1$ and for an obstructed network, it gives how the response of the network deviates from the unobstructed one. Notice that $\chi_1(\omega) = 1$ just for a network of equal vessels, in which K and A do not depend on the level.

The second relation can be obtained by applying eq. (1) at the inlet and the outlet of the network and making the difference of flows.

$$\hat{q}_N^{out} - \hat{q}_1^{in} = -i\omega(\frac{C_N}{k_{cN}^2}\nabla\hat{p}_N^{out} - \frac{C_1}{k_{c1}^2}\nabla\hat{p}_1^{in}) \tag{18}$$

Eq. (18) leads to a second definition of the response of the network: $\chi_2(\omega) = -\frac{\hat{q}_N^{out}-\hat{q}_1^{in}}{i\omega(\frac{C_N}{k_{cN}^2}\nabla\hat{p}_N^{out}-\frac{C_1}{k_{c1}^2}\nabla\hat{p}_1^{in})}$